

CDF Hot Topics

D. Tonelli (for the CDF Collaboration)

I.N.F.N. Sezione di Pisa - Ed. C, Polo Fibonacci, Largo B. Pontecorvo, 3 - 56127 Pisa, Italy

After an introduction on the peculiarities of flavor-physics measurements at a hadron collider, and on the upgraded Collider Detector at Fermilab (CDF II), I show recent results on two-body B^0 and B_s^0 decays into charged, pseudo-scalar, charmless mesons or into muons, to illustrate how the flavor physics program at CDF is competitive with (in B^0 decays) and complementary (in B_s^0 decays) to B -factories. Results shown include the new measurement of the CP-violating asymmetry in $B^0 \rightarrow K^+\pi^-$ decays, the first measurement of the time-evolution of $B_s^0 \rightarrow K^+K^-$ decays, and the world best limits on the decay rates of rare $B_{(s)}^0 \rightarrow \mu^+\mu^-$ modes.

1. Introduction

Precise measurements in B^0 and B^+ meson decays, performed in recent years at the B -factories, provided several substantial improvements in understanding flavor dynamics. However, several open questions remain, and a continuous experimental effort is still necessary to complete the picture. In this respect, simultaneous access to decays of strange and non-strange b -mesons, an opportunity that is currently unique to the Tevatron¹, might simplify the extraction of quark flavor-mixing (CKM) parameters in measurements affected by sizable hadronic uncertainties.

I focus here on the recent CDF results on two-body $B_{(s)}^0$ decays into charmless, charged pseudo-scalar mesons or into muons. These results show how CDF program is becoming fully competitive with B -factories in untagged, time-independent analyses of B^0 meson decays into charged final states, and complementary to B -factories in analyses of B_s^0 modes.

Unless otherwise stated, \mathbf{C} -conjugate modes are implied throughout this paper, and branching-fractions (\mathcal{B}) indicate CP-averages. In addition, the first uncertainty associated to any number is statistical, and the second one is systematic.

2. CDF II at the Tevatron collider

The analyses presented here used data corresponding to time-integrated luminosities of $\int \mathcal{L} dt \simeq 360\text{--}780 \text{ pb}^{-1}$, collected by the upgraded Collider Detector (CDF II) at the Fermilab Tevatron Collider.

¹After a short test-run, the Belle Collaboration is considering the opportunity to run at the $\Upsilon(5S)$ resonance in the near future; in this case, they will have access to large samples of B_s^0 meson decays as well.

2.1. The Tevatron collider

The Tevatron is a superconducting proton-synchrotron at the final stage of the Fermilab accelerator complex. In Run II (mid-2001–present), it accelerates 36 bunches of protons against 36 bunches of anti-protons producing one crossing every 396 ns at $\sqrt{s} = 1.96 \text{ TeV}$. Since the interaction region is about 30 cm long (r.m.s.) along the beam-line, a properly designed silicon micro-vertex detector is required to ensure good coverage for charged particles. The transverse beam-width at the collision point is about 25–30 μm (r.m.s.), sufficiently small with respect to the typical transverse decay-length² of b -hadrons, $L_{xy} \simeq 450 \mu\text{m}$, to allow separation of secondary from primary vertices. The instantaneous luminosity (\mathcal{L}) has been rising steadily during Run II up to the world record peak of $\mathcal{L} \simeq 1.82 \times 10^{32} \text{ cm}^{-2}\text{s}^{-1}$, and regularly exceeds $\mathcal{L} = 10^{32} \text{ cm}^{-2}\text{s}^{-1}$; at such luminosities, two $p\bar{p}$ interactions per bunch-crossing occur on average. The machine typically delivers data corresponding to $\int \mathcal{L} dt \simeq 20 \text{ pb}^{-1}$ per week, which are recorded with average data-taking efficiencies in excess of 85% at CDF. As of May 2006, the total luminosity gathered on tape is around 1.4 fb^{-1} , of which approximately 1 fb^{-1} was recorded with all crucial sub-detectors for flavor-physics operative.

2.2. The CDF II detector

The CDF II detector is a 5000 t, multipurpose, solenoidal magnetic-spectrometer surrounded by 4 π calorimeters and muon detectors; it is axially and azimuthally symmetric around the interaction point. Its excellent tracking performance, good muon coverage, and particle identification (PID) capabilities allow a broad flavor-physics program. We briefly outline the

² $L_{xy} = \beta_T \gamma c \tau$, with typical Lorentz boost projected onto the plane perpendicular to the beam-line $\beta_T \gamma \simeq 0.5\text{--}2$, and typical pseudo-proper decay-length of the b -hadron $c\tau \simeq 450 \mu\text{m}$.

sub-detectors pertinent to the analyses described here, additional details can be found elsewhere [1, 2].

The CDF II tracking system consists of an inner silicon system surrounded by a cylindrical gas-wire drift chamber, both immersed in a 1.4 T solenoidal magnetic field with 135 cm total lever arm. Six (central region, $|\eta| < 1$) to seven (forward, $1 < |\eta| < 2$) double-sided silicon layers, plus one single-sided layer, extend radially from 1.6 to 22 cm (28 cm) from the beam line in the central (forward) region, fully covering the luminous region. The chamber provides 96 (48 axial and 48 stereo) samplings of charged-particle paths between 40 and 137 cm from the beam, and within $|\eta| < 1$. The long lever-arm of the tracker provides a superb mass-resolution: with $\sigma_{p_T}/p_T^2 < 0.15\%(\text{GeV}/c)^{-1}$, typical observed mass-widths are about 14 MeV/ c^2 for $J/\psi \rightarrow \mu^+\mu^-$ decays, and about 9 MeV/ c^2 for $D^0 \rightarrow K^-\pi^+$ decays. In addition, silicon measurements close to the beam allow precise reconstruction of decay vertices, with typical resolutions of 30 μm in the transverse plane and 70 μm along the beam direction.

Four layers of planar drift chambers detect muon candidates with $p_T > 1.4$ GeV/ c in the $|\eta| < 0.6$ region, while conical sections of drift tubes extend the coverage to $0.6 < |\eta| < 1.0$ for muon candidates with $p_T > 2.0$ GeV/ c . Low-momentum PID is obtained with a scintillator-based Time-of-Flight detector with about 110 ps resolution, that provides 2σ separation between kaons and pions with $p < 1.5$ GeV/ c . The information of specific energy-loss from the drift chamber (dE/dx) complements the PID with 1.4 σ nearly constant K/π separation for higher-momentum charged particles ($p > 2$ GeV/ c).

2.3. Flavor physics at CDF

Heavy-flavor phenomenology at the Tevatron is different with respect to the e^+e^- environment. A large $p\bar{p} \rightarrow b\bar{b}X$ rate is exploited, which results in a production cross-section of about 30 μb [1] for b -hadrons within detector coverage, compared to 1 nb (7 nb) $e^+e^- \rightarrow b\bar{b}$ cross-sections at the $\Upsilon(4S)$ (Z^0) resonances. Unlike at the B -factories, all species of b -hadrons are produced at the Tevatron, including B_s^0 and B_c^+ mesons, and b -baryons. In addition, the dominant source of b -hadrons is incoherent, strong production of $b\bar{b}$ pairs; thus measurements that require flavor-tagging can be done by reconstructing a single b -hadron in the event, while at B -factories the flavor of one b -meson is determined only after observing the decay of the other one.

However, the $p\bar{p}$ collider poses also several challenges. The large $b\bar{b}$ production cross-section is still only about $1/1000^{\text{th}}$ the total inelastic $p\bar{p}$ cross-section. Moreover, high (≈ 30) track multiplicities per event are observed at the Tevatron, owing to frag-

mentation of the hard-interaction products, to the underlying events (i. e., hadronized remnants of p and \bar{p}) and to pile-up events (multiple collisions per bunch crossing). In addition, the transverse momentum distribution of b -hadrons is a rapidly falling function: most b -hadrons have low- p_T and decay into particles which are typically quite soft, often having $p_T < 1$ GeV/ c ; thus, the need to select low- p_T particles conflicts with the limited bandwidth allowed by the data acquisition systems; furthermore, since the longitudinal component of b -hadron momenta is frequently large, their decay-products tend to be boosted along the beam line, thus escaping the detector acceptance. If one b -quark is within CDF acceptance, the other one is within acceptance only $\mathcal{O}(10\%)$ of the time.

The best way to identify b -flavor decays in such a challenging environment is to exploit their relatively long lifetime, which results in decay vertices separated by hundreds of microns from the $p\bar{p}$ interaction, for hadrons with typical boosts. In this respect, CDF excellent tracking plays a key role for an effective b -hadron reconstruction; equally important is its highly-specialized and selective trigger, which uses silicon tracking information online and gathers large and pure samples of *charmed* and *beauty* decays while sustaining the high-rates associated with the $p\bar{p}$ environment.

2.4. Role of trigger

CDF exploits its unique ability to trigger events with charged particles originated in vertices displaced from the primary $p\bar{p}$ vertex (displaced tracks) [3]. Displaced tracks are identified by measuring with 35 μm intrinsic resolution³ their impact parameter, which is the minimum distance between the particle direction and the primary $p\bar{p}$ vertex in the plane transverse to the beam. Such a high accuracy can be reached only using online the silicon information, a challenging task that requires to read-out 212,000 silicon channels and to complete hit-clustering and pattern recognition within the trigger latency. In a highly-parallelized architecture, fast pattern-matching and linearized track-fitting allow reconstruction of 2D-tracks in the plane transverse to the beam with offline-quality by combining drift-chamber and silicon information, within a typical latency of 25 μs per event.

Using the above device, CDF implemented a trigger selection that requires only two displaced tracks in the event, to collect pure samples of exclusive non-leptonic b -decays for the first time in a hadron collider e. g., $B^0 \rightarrow \pi^+\pi^-$ and $B_s^0 \rightarrow D_s^-\pi^+$ decays, in addition to

³The intrinsic resolution combined with the beam-width $\sigma_{\text{beam}} \simeq 30$ μm determines the total impact parameter resolution, $\sigma_{\text{SVT}} \oplus \sigma_{\text{beam}} \simeq 47$ μm .

large samples of semileptonic b -decays and of *charmed* meson decays. However, an impact-parameter based selection biases the decay-length distributions, reducing the statistical power in lifetime measurements. In section 3.2 we discuss how the original lifetime information is deconvolved from the trigger efficiency, and from the smearing effects due to the finite resolution on the measured impact parameters and decay lengths.

Besides the trigger on displaced tracks, past experience from Run I suggests that triggering on final states containing single or dileptons is a successful strategy to select samples of b -hadron decays, because semileptonic ($B \rightarrow \ell \nu_l X$) and *charmonium* ($B \rightarrow J/\psi X \rightarrow [l^+ l^-] X$) decays represent about 20% of b -meson widths and have relatively clean experimental signatures. Such a ‘conventional’ approach was adapted to the upgraded detector: identification of muon down to low momenta allows for efficient dimuon triggers in which we select *charmonium* or rare decays and then we fully reconstruct several decay modes. On the other hand, semileptonic triggers require a displaced track in addition to the muon (or electron), providing cleaner samples.

3. Analysis of $B_{(s)}^0 \rightarrow h^+ h'^-$ decays

The extraction of CKM parameters from measurements in b -hadron decays is often affected by large uncertainties, coming from non-perturbative QCD effects. One way to simplify the problem is to invoke flavor-symmetries under which the unknowns partially cancel. In this respect, joint study of B^0 and B_s^0 two-body decays into charged kaons and pions ($B_{(s)}^0 \rightarrow h^+ h'^-$) plays a key role, since these modes are related by subgroups of the SU(3) symmetry [4, 5, 6]. CDF is the only experiment, to date, that has simultaneous access to these modes; this provides a rich flavor-physics program: the analysis of first Run II data already lead to the first observation of $B_s^0 \rightarrow K^+ K^-$ decays, and to the world best limits on $B_s^0 \rightarrow K^- \pi^+$ and $B_s^0 \rightarrow \pi^+ \pi^-$ decay rates [7, 8]; now, with samples increased in size, CDF is approaching the opportunity to obtain competitive measurements of CP-violating phases.

3.1. CP asymmetry in $B^0 \rightarrow K^+ \pi^-$ decays

The flavor-specific⁴ $B^0 \rightarrow K^+ \pi^-$ decay occurs in the standard model (SM) through the dominant ‘tree’ (of amplitude T) and ‘penguin’ (P) diagrams.

Their interfering amplitudes induce the CP asymmetry $A_{CP}(B^0 \rightarrow K^+ \pi^-)$ defined as follows:

$$\begin{aligned} & \frac{\mathcal{B}(\bar{B}^0 \rightarrow K^- \pi^+) - \mathcal{B}(B^0 \rightarrow K^+ \pi^-)}{\mathcal{B}(\bar{B}^0 \rightarrow K^- \pi^+) + \mathcal{B}(B^0 \rightarrow K^+ \pi^-)} \\ &= \frac{2|T||P|\sin(\delta)\sin(\gamma)}{|T|^2 + |P|^2 + 2|T||P|\cos(\delta)\cos(\gamma)}, \end{aligned} \quad (1)$$

which is sensitive to the V_{ub} CKM phase (angle $\gamma \equiv \phi_3$) and to the difference δ between strong phases of the two amplitudes. B -factories recently measured a $\mathcal{O}(10\%)$ asymmetry with 2% accuracy, probing for the first time direct CP violation in the b -quark sector [9, 10]; however, additional experimental information is needed because theoretical predictions still suffer from large (5–10%) uncertainties [11, 12, 13], and the observed asymmetries in neutral and charged modes are not consistent, as the SM would suggest. A measurement from the Tevatron is therefore interesting, also for the unique possibility to combine asymmetry measurements in $B^0 \rightarrow K^+ \pi^-$ and $B_s^0 \rightarrow K^- \pi^+$ decays, which provide a model-independent probe for the presence of non-SM physics [14].

We analyzed a $\int \mathcal{L} dt \simeq 360 \text{ pb}^{-1}$ sample of pairs of oppositely-charged particles, used to form $B_{(s)}^0$ meson candidates, with $p_T > 2 \text{ GeV}/c$ and $p_T(1) + p_T(2) > 5.5 \text{ GeV}/c$. The trigger required also a transverse opening-angle between tracks $20^\circ < \Delta\phi < 135^\circ$ to reject background from particles within light-quark jets. In addition, both charged particles were required to originate in a displaced vertex ($100 \mu\text{m} < d_0 < 1 \text{ mm}$), while the $B_{(s)}^0$ meson candidate was required to be produced in the primary $p\bar{p}$ interaction ($d_0(B) < 140 \mu\text{m}$) and to have travelled a transverse distance $L_{xy}(B) > 200 \mu\text{m}$.

A $B_{(s)}^0 \rightarrow h^+ h'^-$ signal of about 3800 events and signal-to-noise ratio $\text{SNR} \simeq 0.2$ at peak is visible in data (Fig. 1, left) already after confirming the trigger selection on offline quantities: extraction of a $\mathcal{B} \simeq 10^{-5}$ signal at trigger-level is a remarkable achievement at a hadron collider, made it possible by the CDF trigger on displaced tracks.

In the offline analysis, an unbiased procedure of optimization determined a tightened selection on track-pairs fit to a common decay-vertex. We found the optimal selection by minimizing the following analytical parameterization of the average expected resolution on the asymmetry measurement: $\sigma_{A_{CP}} = \frac{1}{\sqrt{S}} \sqrt{z + w(B/S)}$. For each set of cuts, S was the signal yield, estimated from Monte Carlo simulation and normalized to the yield observed in data after the trigger selection, and B were the background events found in the sidebands of the $\pi\pi$ -mass distribution in data. The constants w and z were parameters determined *a priori* from full analyses of pseudo-experiments reproducing the experimental circumstance of data. By using $\sigma_{A_{CP}}$ we obtained about 10% improvement in res-

⁴We neglect the $\mathcal{O}(10^{-4})$ fraction of doubly-Cabibbo suppressed decays.

olution over the standard $\sqrt{S+B}/S$. Besides tightening the trigger cuts, in the analysis we exploited the discriminating power of the $B_{(s)}^0$ meson ‘isolation’ and of the information provided by the 3D reconstruction capability of CDF tracking, which both allowed great improvement in signal purity. Isolation was defined as $I(B) = p_T(B)/[p_T(B) + \sum_i p_T(i)]$, in which the sum runs over every other track within a cone of radius one in the $\eta - \phi$ space around the $B_{(s)}^0$ meson flight-direction; by requiring $I(B) > 0.5$, we reduced the background by a factor four while keeping almost 80% of signal. The 3D view of tracking allowed to resolve multiple vertices along the beam direction reducing the background (mainly pairs of displaced tracks coming from distinct, uncorrelated heavy-flavor decays) by a factor two, with little inefficiency on signal.

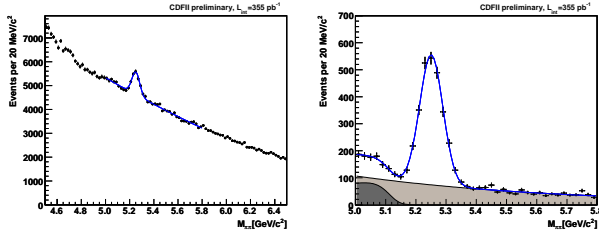


Figure 1: Invariant $\pi\pi$ -mass after the trigger (left plot) and after the optimized offline selection (right plot). Latter plot shows also background contributions from random pairs of tracks which satisfy the selection requirements (light gray) and partially-reconstructed $B_{(s)}^0$ meson decays (dark gray), as resulting from the invariant-mass fit.

The resulting $\pi\pi$ -mass distribution (Fig. 1, right) shows a clean signal, estimated by a Gaussian (signal) plus an exponential (combinatoric background) and an Argus-shaped (physics background) fit to contain 2327 ± 77 events, with standard deviation $\sigma = 39 \pm 1$ MeV/ c^2 and $\text{SNR} \simeq 6.5$ at peak. This corresponds to a factor 1.7 reduction in signal yield and to a factor of 50 reduction in background with respect to the trigger selection (Fig. 1, left).

Despite the excellent mass resolution, the various $B_{(s)}^0 \rightarrow h^+ h'^-$ modes overlapped into an unresolved mass peak, while the PID resolution was insufficient for separating them on an event-by-event basis. We achieved a statistical separation instead, with a multivariate, unbinned likelihood-fit (fit of composition) that used PID information, provided by the dE/dx in the drift chamber, and kinematics.

We exploited the kinematic differences among modes by using an approximate relation between any two invariant masses (M_{m_1, m_2} and $M_{m'_1, m'_2}$) obtained with two arbitrary mass-assignments to the outgoing particles (m_1, m_2 and m'_1, m'_2). If $m_{1,2} \ll p_{1,2}$ we have

$$M_{m_1, m_2}^2 \approx M_{m'_1, m'_2}^2 + (1 + p_1/p_2) \cdot (m_2^2 - m_2'^2) + (1 + p_2/p_1) \cdot (m_1^2 - m_1'^2) \quad (2)$$

where kinematic information associated to all possible mass-assignments ($K^+\pi^-, K^-\pi^+, \pi^+\pi^-, K^+K^-$) was compacted within just two observables, a single candidate invariant-mass and the ratio of momenta. Left plot in Fig. 2 shows the averaged $\pi\pi$ -mass as a function of the signed momentum-imbalance, $\alpha = (1 - p_1/p_2)q_1$, for simulated $B^0 \rightarrow K^+\pi^-$ and $\bar{B}^0 \rightarrow K^-\pi^+$ events. The momentum (charge) p_1 (q_1) refers to the softer track; by combining kinematics and charge, we therefore separated also $K^+\pi^-$ from $K^-\pi^+$ final states.

We equalized the dE/dx over the tracking volume and time using about 760,000 $D^{*+} \rightarrow D^0\pi^+ \rightarrow [K^-\pi^+]\pi^+$ decays, where identity of D^0 daughters was tagged by the strong D^{*+} decay [15]. The $\mathcal{O}(0.4\%)$ contamination from doubly Cabibbo-suppressed $D^0 \rightarrow K^+\pi^-$ decays was neglected. In a $> 95\%$ pure D^0 sample, we obtained 1.4σ separation between kaons and pions (Fig. 2, right), corresponding to an uncertainty on the measured fraction of each class of particles that is just 60% worse than the uncertainty attainable with ideal separation. We measured, and included in the fit, a 11% residual track-to-track correlation due to common-mode dE/dx fluctuations.

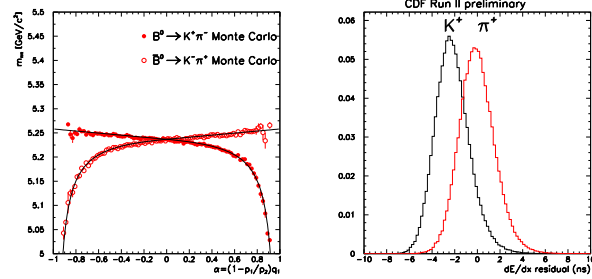


Figure 2: Averaged $m_{\pi\pi}$ distribution as a function of the signed momentum imbalance (α) for simulated $B^0 \rightarrow K^+\pi^-$ and $\bar{B}^0 \rightarrow K^-\pi^+$ events with analytical function of Eq. (2) overlaid (left plot); distribution of the difference between observed dE/dx and expected dE/dx (in pion mass-hypothesis) for positive kaons and pions (right plot).

The fit of composition used five observables: the invariant $\pi\pi$ -mass $m_{\pi\pi}$, the signed momentum-imbalance α , the scalar sum of particles' momenta p_{tot} , and the dE/dx of both particles. The likelihood for the single event i was $\mathcal{L}^i = (1 - b) \sum_j f_j \mathcal{L}_j + b \mathcal{L}_{\text{bck}}$, where j runs over the signal modes, and f_j (b) are the fractions of each mode (background) to be determined by the fit. In terms of probability density functions (p.d.f.), each term of the likelihood reads as

$$\mathcal{L} \simeq \wp^m(m_{\pi\pi}|\alpha) \wp^p(\alpha, p_{\text{tot}}) \wp^{\text{PID}}(dE/dx_1, dE/dx_2). \quad (3)$$

The mass (\wp^m) model was obtained from the analytical formula Eq. (2) for signal and from mass-sidebands of data for background; the momentum term (\wp^p) was

derived from simulation for signal and from mass-sidebands of data for background. The PID term (ϕ^{PID}) was extracted from calibration samples of D^0 decays for signal and background.

The fit found three modes that contribute to the peak: $313 \pm 34 B^0 \rightarrow \pi^+\pi^-$, $1475 \pm 60 B^0 \rightarrow K^+\pi^-$, and $523 \pm 41 B_s^0 \rightarrow K^+K^-$ decays. A not yet statistically significant contribution of $64 \pm 30 B_s^0 \rightarrow K^-\pi^+$ decays was also found. Fit projections are overlaid to data in Fig. 3.

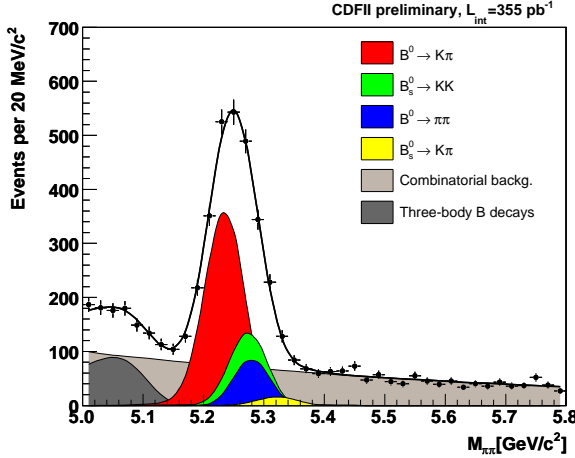


Figure 3: Invariant $\pi\pi$ -mass after the offline selection with individual signal components (cumulative) and backgrounds (overlapping) overlaid.

From 787 ± 42 reconstructed $B^0 \rightarrow K^+\pi^-$ decays and 689 ± 41 reconstructed $\bar{B}^0 \rightarrow K^-\pi^+$ decays, we measured the following uncorrected value for the direct CP asymmetry:

$$\frac{N(\bar{B}^0 \rightarrow K^-\pi^+) - N(B^0 \rightarrow K^+\pi^-)}{N(\bar{B}^0 \rightarrow K^-\pi^+) + N(B^0 \rightarrow K^+\pi^-)} = (-6.6 \pm 3.9)\%. \quad (4)$$

Above result was then corrected for differences in trigger, reconstruction, and selection efficiencies between $B^0 \rightarrow K^+\pi^-$ and $\bar{B}^0 \rightarrow K^-\pi^+$ modes; since the known, small ($< 2\%$) detector charge-asymmetry canceled out almost completely in this measurement, the only effect that mattered was the different probability of interaction with the beam-pipe and tracker material between positive and negative kaons. This required a $(1.00 \pm 0.25)\%$ correction to the observed asymmetry. The value of the correction was extracted from simulation and checked in unbiased kaons from $D^+ \rightarrow K^-\pi^+\pi^+$ decays triggered on the pion pair. The corrected CP asymmetry in $B^0 \rightarrow K^+\pi^-$ decay-rates is therefore $A_{\text{CP}}(B^0 \rightarrow K^+\pi^-) = (-5.8 \pm 3.9)\%$.

The various contributions to the systematic uncertainty, evaluated with pseudo-experiments, sum to a total uncertainty of 0.7% , still smaller than the statistical uncertainty. The dominant source was the

uncertainty on the dE/dx model for kaons, pions, and track-to-track correlation. This effect is expected to partially reduce as the size of calibration samples of D^0 decays increases. The second important contribution derived from the statistical uncertainty on the nominal value of $B_{(s)}^0$ meson masses, which enters in the analytical expression Eq. (2). Since we use the $B_{(s)}^0$ meson masses measured by CDF, this uncertainty will reduce with the increasing statistic of fully-reconstructed $B_{(s)}^0$ meson decays. Other relevant contributions came from the uncertainty on the invariant-mass resolution for each $B_{(s)}^0 \rightarrow h^+h'^-$ mode, from possible shifts of the global mass scale with respect to nominal masses, from possible charge-asymmetries in background that could fake an asymmetry in $B^0 \rightarrow K^+\pi^-$ rates, and from the uncertainty on the invariant-mass shape assumed for the combinatoric background.

We quote the following result for the direct CP asymmetry in $B^0 \rightarrow K^+\pi^-$ decays, where all contributions to the systematic uncertainty have been summed in quadrature:

$$A_{\text{CP}}(B^0 \rightarrow K^+\pi^-) = (-5.8 \pm 3.9 \pm 0.7)\%, \quad (5)$$

which is approximately 1.5σ different from zero, and in agreement with world best results: $A_{\text{CP}}(B^0 \rightarrow K^+\pi^-) = (-11.3 \pm 2.2 \pm 0.8)\%$, from the Belle Collaboration [10], and $A_{\text{CP}}(B^0 \rightarrow K^+\pi^-) = (-13.3 \pm 3.0 \pm 0.9)\%$ from the Babar Collaboration [9].

CDF result is still limited by the statistic uncertainty; however, its systematic uncertainty, at the same level of B -factories, is promising: with significantly more data already collected, we expect to reduce the statistical uncertainty down to 2.5% , which will make CDF result competitive with B -factories soon.

3.2. Time-evolution of $B_s^0 \rightarrow K^+K^-$ decays

The recent, first result on the B_s^0 flavor-oscillation frequency by CDF [16] is consistent with SM predictions. The SM predicts the mass difference between CP eigenstates⁵ Δm_s to be related to the width difference $\Delta\Gamma_s$ by the relation $\Delta\Gamma_s/\Delta m_s \simeq 0.003$ [17]; hence an observed $\Delta\Gamma_s$ inconsistent with above ratio would hint at non-SM, CP-violating, new phases. A way to probe $\Delta\Gamma_s$ is to measure the lifetime of CP-specific B_s^0 decays, and to combine it with the lifetime in flavor-specific decays to extract $\Delta\Gamma_s/\Gamma_s$.

⁵As usually allowed in the SM, we neglect the mixing phase $-2\beta_s$, thus mass and CP eigenstates coincide.

In the same $\int \mathcal{L} dt \simeq 360 \text{ pb}^{-1}$ sample used for the asymmetry measurement, we measured the time-evolution of untagged $B_s^0 \rightarrow K^+ K^-$ decays, which are expected to be 95% CP-even eigenstates. A similar unbiased optimization procedure, aimed at improving the resolution on lifetime-measurements, yielded an offline-selection based on transverse-momentum, impact-parameter, and vertex-quality requirements. The resulting signal was similar to the one shown in right plot of Fig. 1, and contained about 2200 $B_{(s)}^0 \rightarrow h^+ h'^-$ decays, with 5.0 approximate peak SNR.

The time-evolution of individual signal modes was determined by adding the decay-length information to the fit of composition described in the previous section. We multiplied the p.d.f. of Eq. (3) by the following lifetime-term:

$$\phi^{\text{life}}(ct) = [\exp(ct) \otimes \mathcal{G}(\sigma_{ct})] \times \epsilon(ct), \quad (6)$$

in which the exponential modeled the evolution of the decay, the second term accounted for a Gaussian detector-smearing that depended on the event-by-event uncertainty (σ_{ct}), and the third term was an efficiency that depended on the decay length and accounted for the lifetime bias. The bias of the lifetime distribution due to resolution and efficiency effects introduced by the trigger on displaced vertices, and by the offline analysis, was modeled with a unique efficiency curve $\epsilon(ct)$. This was defined as the ratio between the pseudo-proper decay length distribution of events passing the trigger and the unsculpted one, and it was extracted from simulated samples. We checked the agreement of simulation with real data, and we verified that the efficiency curves were independent of the lifetime of the simulated samples used to derive them. A standard lifetime-fit was performed on $B^+ \rightarrow J/\psi K^+$ decays, which were collected by the dimuon trigger, and therefore were free from any lifetime bias; then we applied offline the selection of the displaced-track trigger to these decays to select a ‘lifetime-biased’ sub-sample; the lifetime of this sub-sample was fit using an efficiency curve extracted by the simulation, and was found in good agreement with the unbiased lifetime of the whole sample. In addition, distinct samples of $B^+ \rightarrow \bar{D}^0 \pi^+$ were simulated with different lifetimes; an efficiency curve was extracted for each sample, and was applied to a different lifetime-fit in data; no dependence on the $c\tau$ of the simulated sample was found in the resulting lifetimes in data. The efficiency curve of the $B_s^0 \rightarrow K^+ K^-$ mode is shown in Fig. 4.

The addition of lifetime information in the fit did not biased the estimated signal composition, which was found in good agreement with what obtained in the previous section. The estimated pseudo-proper decay-lengths were $c\tau(B^0) = 452 \pm 24 \mu\text{m}$ for the B^0 meson, and $c\tau(B_s^0 \rightarrow K^+ K^-) = 463 \pm 56 \mu\text{m}$

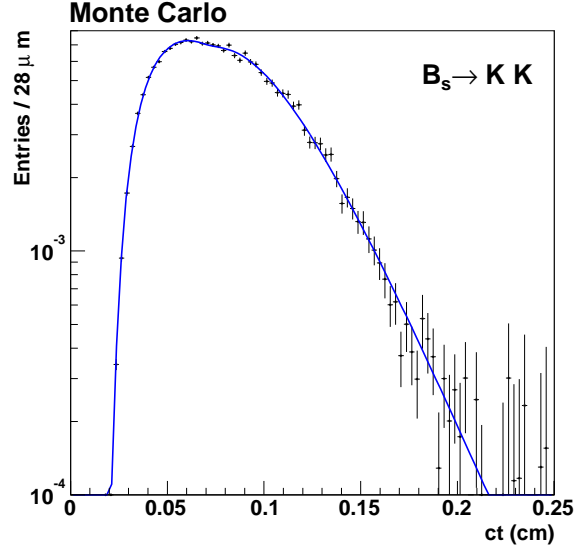


Figure 4: Combined trigger and selection efficiency for the $B_s^0 \rightarrow K^+ K^-$ mode as a function of the decay length.

for the $B_s^0 \rightarrow K^+ K^-$ decay. We assumed the time-evolution of the $B_s^0 \rightarrow K^+ K^-$ decay to be a single-exponential i. e., $B_s^0 \rightarrow K^+ K^-$ was assumed to be a pure CP-even eigenstate.

With a Gaussian constraint on the B^0 meson lifetime to the world average value [18], we obtained $c\tau(B_s^0 \rightarrow K^+ K^-) = 458 \pm 53 \mu\text{m}$. The lifetime distribution of the signal with fit projection overlaid is shown in Fig. 5.

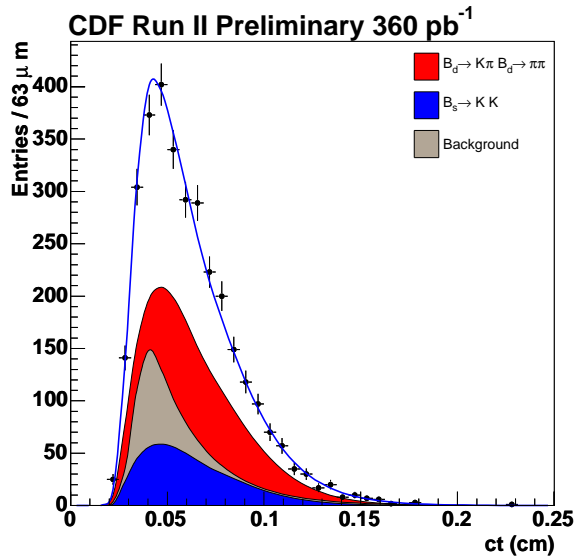


Figure 5: Lifetime distribution of signal events (dots) with fit projections overlaid.

The total systematic uncertainty was $5.6 \mu\text{m}$, significantly smaller than the statistic uncertainty. Its

dominant sources included the effect of misalignments in the tracker, the uncertainties on the model used for proper-time resolution and for the lifetime of background, the uncertainty on the dE/dx model, the uncertainty on the input $p_T(B)$ spectrum used in the simulation, and the uncertainty on the extraction of the trigger-efficiency curve. The resulting $B_s^0 \rightarrow K^+ K^-$ lifetime was

$$\tau_L = 1.53 \pm 0.18 \pm 0.02 \text{ ps}, \quad (7)$$

which, combined with the world average flavor-specific B_s^0 meson lifetime [19], yielded the following measurement of the width-difference in the B_s^0 -system for CP-eigenstates:

$$\frac{\Delta\Gamma_s^{\text{CP}}}{\Gamma_s^{\text{CP}}} = -0.08 \pm 0.23 \pm 0.03. \quad (8)$$

This result, still limited by statistical uncertainty, is already the second world best measurement; an uncertainty at the 0.10 level is expected with the upcoming upgrade of the analysis to the data already collected.

4. Search for the rare $B_{(s)}^0 \rightarrow \mu^+ \mu^-$ decays

In the SM, Flavor Changing Neutral Current (FCNC) decays are strongly suppressed; for instance, the expected branching-fractions of rare $B_{(s)}^0 \rightarrow \mu^+ \mu^-$ decays are around 3.4×10^{-9} for the B_s^0 mode [20, 21], and approximately 1×10^{-10} [20] for the B^0 mode, further suppressed by a factor $|V_{td}/V_{ts}|^2$. Above rates are a factor $\mathcal{O}(100)$ beyond current experimental sensitivity at the Tevatron. However, contribution from non-SM physics may significantly enhance these rates, making it possible an observation that would be unambiguous signature for new physics.

In minimal supersymmetric (SUSY) extensions of the SM, for instance, additional processes involving virtual SUSY particles imply $\mathcal{B}(B_{(s)}^0 \rightarrow \mu^+ \mu^-) \propto \tan^6(\beta)$; $\tan(\beta)$ is the ratio of vacuum expectation values of the two neutral CP-even Higgs fields; hence large enhancements of the decay rate are expected in those SUSY models, like minimal SO(10) [22, 23, 24, 25], that favor higher values of $\tan(\beta)$ [26, 27, 28]. On the other hand, R-parity violating SUSY models [28] may enhance $B_{(s)}^0 \rightarrow \mu^+ \mu^-$ rates even at lower values of $\tan(\beta)$. Hence, while an observation of $B_{(s)}^0 \rightarrow \mu^+ \mu^-$ decays would provide crucial information on the flavor-structure of new physics, even improved exclusion-limits constrain the available space of parameters of several SUSY models.

We searched for $B_{(s)}^0 \rightarrow \mu^+ \mu^-$ decays in $\int \mathcal{L} dt \simeq 780 \text{ pb}^{-1}$ of data collected by two dimuon triggers: one that required both muon candidates in the $|\eta| < 0.6$ region (U-U channel), the other that required

one muon candidate in the $0.6 < |\eta| < 1.0$ region (U-X channel). The offline selection required two oppositely-charged muon candidates fit to a common decay-vertex. We cut on the dimuon transverse momentum to reject combinatoric background, on the 3D decay-length (λ) and on its resolution to reject prompt background, and on the isolation of the $B_{(s)}^0$ meson candidate to exploit the harder fragmentation of b -mesons with respect to light-quark background; in addition, we required the candidate to point back to the primary vertex to further reduce combinatoric background and partially reconstructed b -hadron decays. The final sample contained about 23,000 candidates, mostly coming from random combinatoric background. Distributions of the discriminating observables for signal (detailed simulation) and background (data) are shown in Fig. 6.

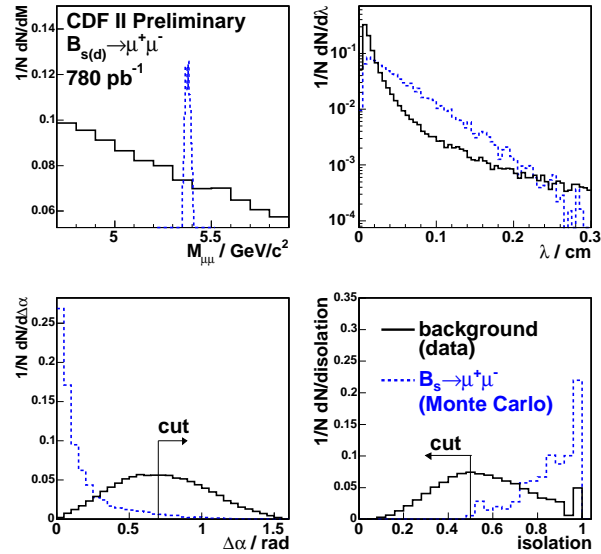


Figure 6: Distribution of the discriminating observables for data, dominated by background (solid histogram), and simulated $B_s^0 \rightarrow \mu^+ \mu^-$ decays (dashed histogram).

To further enhance purity we applied a cut on a likelihood-ratio (LR) variable based on three input observables: the isolation of the candidate, its decay-length probability ($e^{-ct/c\tau}$), and its ‘pointing’ to the primary vertex (i. e., the opening angle $\Delta\alpha$ between the $p_T(B)$ -vector and the vector of the displacement between the $p\bar{p}$ vertex and the decay-vertex of the candidate). We extracted the signal p.d.f. from detailed simulation and the background p.d.f. from mass-sidebands in data. Distributions of LR for signal and background are shown in Fig. 7.

The $B_{(s)}^0 \rightarrow \mu^+ \mu^-$ branching-fractions were obtained by normalizing to the number of $B^+ \rightarrow J/\psi K^+ \rightarrow [\mu^+ \mu^-] K^+$ decays collected in the same sample. The ratio of trigger acceptances between signal and normalization modes ($\simeq 25\%$) was derived

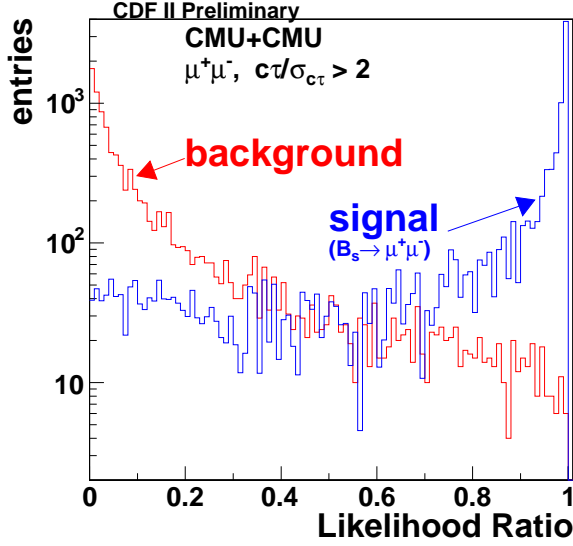


Figure 7: Distribution of LR for data mass-sidebands (red histogram), and simulated signal (blue histogram).

from simulation, the relative trigger efficiencies ($\simeq 1$) were extracted from unbiased data and the relative offline-selection efficiency ($\simeq 90\%$) was determined from simulation.

The expected average number of background events was obtained by extrapolating events from the mass-sidebands to the search boxes. This estimate was checked by comparing predicted and observed background yields in the following control samples: like-sign dimuon candidates, opposite-sign dimuon candidates with negative decay-length, and opposite-sign dimuon candidates in which one muon failed the muon-quality requirements. Contributions of punch-through hadrons from $B_{(s)}^0 \rightarrow h^+ h'^-$ decays were included in the estimate of total background. The optimal value for the LR cut was obtained by searching for the *a priori* best expected 90% C.L. upper limit on $\mathcal{B}(B_{(s)}^0 \rightarrow \mu^+ \mu^-)$. In two, 120 MeV/ c^2 -wide search windows (to be compared with 25 MeV/ c^2 mass-resolution) centered at the world average $B_{(s)}^0$ meson masses, we found 1 (0) and 2 (0) events in the U-U (U-X) channel for B_s^0 and B^0 decays respectively, in agreement with 0.88 ± 0.30 (0.39 ± 0.21) expected background events (see Fig. 8). The resulting combined upper-limits, estimated according to the Bayesian approach of Ref. [18], and assuming a flat prior for the branching-fractions, were the following:

$$\mathcal{B}(B_s^0 \rightarrow \mu^+ \mu^-) < 8.0 \times 10^{-8} \text{ at 90\% C.L.} \quad (9)$$

$$\mathcal{B}(B^0 \rightarrow \mu^+ \mu^-) < 2.3 \times 10^{-8} \text{ at 90\% C.L.,} \quad (10)$$

which became respectively $\mathcal{B}(B_s^0 \rightarrow \mu^+ \mu^-) < 1.0 \times 10^{-7}$ and $\mathcal{B}(B^0 \rightarrow \mu^+ \mu^-) < 3.0 \times 10^{-7}$ at 95% C.L. These results improve by a factor of two previous

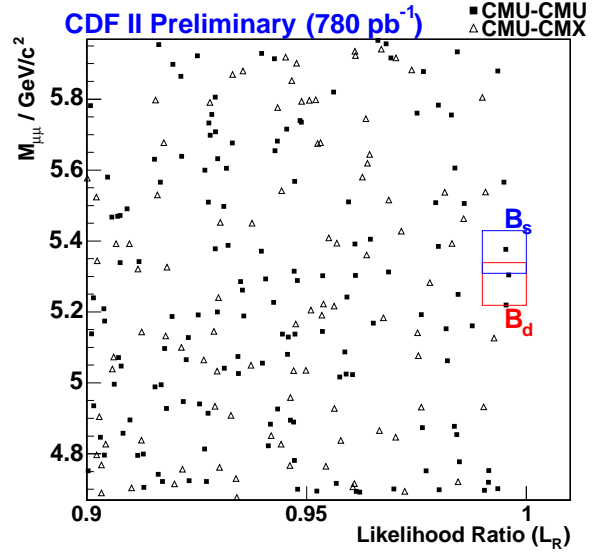


Figure 8: Invariant $\mu^+ \mu^-$ -mass versus LR distribution for events satisfying the offline selection for U-U (solid square) and U-X (open triangle) channels. The B_s^0 (blue box) and B^0 (red box) signal regions are also shown.

limits and significantly reduce the allowed parameter space for a broad range of SUSY models.

5. Summary and outlook

We used $\int \mathcal{L} dt \simeq 360 \text{ pb}^{-1}$ of data collected by the upgraded Collider Detector (CDF II) at the Fermilab Tevatron collider to measure the following CP-violating asymmetry in $B^0 \rightarrow K^+ \pi^-$ decays: $A_{CP}(B^0 \rightarrow K^+ \pi^-) = (-5.8 \pm 3.9 \pm 0.7)\%$ in agreement with the B -factories, and with comparable systematic uncertainties. In the same sample, the time-evolution of the $B_s^0 \rightarrow K^+ K^-$ decay was measured for the first time, yielding to the following measurement of the relative width-difference: $\Delta\Gamma_s^{\text{CP}}/\Gamma_s^{\text{CP}} = -0.08 \pm 0.23 \pm 0.03$. With $\int \mathcal{L} dt \simeq 1 \text{ fb}^{-1}$ already collected, we expect about 2.5% statistical uncertainty on the asymmetry, and about 0.10 uncertainty on the width-difference, which would place these CDF measurements among world best results. In this significantly larger sample, we also expect a precise measurement of the $B_s^0 \rightarrow K^+ K^-$ rate, and either observation of $B_s^0 \rightarrow K^- \pi^+$, $B_s^0 \rightarrow \pi^+ \pi^-$, $\Lambda_b^0 \rightarrow p K^-$, $\Lambda_b^0 \rightarrow p \pi^-$ decays, or setting world best limits on their rates. The $\int \mathcal{L} dt \simeq 1 \text{ fb}^{-1}$ sample is also the starting point for the time-dependent analysis of flavor-tagged $B_{(s)}^0 \rightarrow h^+ h'^-$ decays, which may allow CDF to measure CP-violating asymmetries in $B_s^0 \rightarrow K^+ K^-$ and $B^0 \rightarrow \pi^+ \pi^-$ decays.

Moreover, CDF quotes the following 90% C.L. limits on the branching-fractions of FCNC, rare $B_{(s)}^0 \rightarrow$

$\mu^+\mu^-$ decays: $\mathcal{B}(B_s^0 \rightarrow \mu^+\mu^-) < 8.0 \times 10^{-8}$ and $\mathcal{B}(B^0 \rightarrow \mu^+\mu^-) < 2.3 \times 10^{-8}$, obtained in the $\int \mathcal{L} dt \simeq 780 \text{ pb}^{-1}$ sample. These are already the world best results, and they contributed to exclude a broad portion of parameter space in several SUSY models.

Acknowledgments

I would like to thank the local organizers for a very enjoyable conference, the other participants for useful discussions, and the colleagues from CDF for helpful suggestion in preparing the talk and this document.

References

- [1] D. Acosta *et al.* (CDF Coll.), “Measurement of the J/ψ meson and b -hadron production cross-section in $p\bar{p}$ collisions at $\sqrt{s} = 1960 \text{ GeV}$ ”, Phys. Rev. D **71**:032001 (2005), [hep-ex/0412071].
- [2] R. Blair *et al.* (CDF Coll.), “The CDF II detector - Technical Design Report”, FERMILAB-PUB-96-390-E (1996).
- [3] W. Ashmanskas *et al.*, “The CDF Silicon Vertex Trigger”, Nucl. Instrum. Meth. **A518**:532 (2004), [physics/0306169].
- [4] I. Dunietz, “Extracting CKM parameters from B Decays”, Argonne Accel. Phys. 1993:0225 and Snowmass B Physics 1993:83 (1993).
- [5] R. Fleischer, “New Strategies to Extract β and γ from $B_d \rightarrow \pi^+\pi^-$ and $B_s \rightarrow K^+K^-$ ” Phys. Lett. B **459**:306 (1999), [hep-ph/9903456].
- [6] R. Fleischer and J. Matias, “Exploring CP Violation through Correlations in $B \rightarrow \pi K$, $B_d \rightarrow \pi^+\pi^-$, $B_s \rightarrow K^+K^-$ Observable Space”, Phys. Rev. D **66**:054009 (2002), [hep-ph/0204101].
- [7] D. Tonelli, “Branching fractions of $B_{(s)}^0 \rightarrow h^+h'^- \text{ modes at CDF}$ ”, PoS HEP2005:258 (2006), [hep-ex/0512024].
- [8] G. Punzi, “Branching fractions and CP asymmetries in $B_{(s)}^0 \rightarrow h^+h'^-$ ”, proceedings of ICHEP 2004, vol. 2* 925 (2005), [hep-ex/0504045].
- [9] B. Aubert *et al.* (BaBar Coll.), “Direct CP Violating Asymmetry in $B^0 \rightarrow K^+\pi^-$ Decays”, Phys. Rev. Lett. **93**:131801 (2004), [hep-ex/0407057].
- [10] K. Abe *et al.* (Belle Coll.), “Improved Measurements of Direct CP Violation in $B \rightarrow K^+\pi^-$, $K^+\pi^0$ and $\pi^+\pi^0$ Decays”, [hep-ex/0507045]; Y. Chao, these proceedings.
- [11] Y. Y. Keum and A. I. Sanda “Possible large direct CP violations in charmless B decays - Summary report on the $pQCD$ Method”, Phys. Rev. D **67**:054009 (2003), [hep-ph/0209014].
- [12] M. Beneke *et al.*, “QCD Factorization in $B \rightarrow \pi K$, $\pi\pi$ Decays and Extraction of Wolfenstein Parameters”, Nucl. Phys. B **606**:245 (2001), [hep-ph/0104110].
- [13] H. N. Li and S. Mishima “On the $B \rightarrow \pi\pi$ puzzle”, [hep-ph/0602214].
- [14] H. J. Lipkin, “Is observed direct CP violation in $B_d \rightarrow K^+\pi^-$ due to new physics? Check standard model prediction of equal violation in $B_s \rightarrow K^-\pi^+$ ”, Phys. Lett. B **621**:126 (2005), [hep-ph/0503022].
- [15] D. Tonelli, Ph.D. Thesis, Scuola Normale Superiore, Pisa (in preparation).
- [16] G. Gomez-Ceballos and J. Piedra, these proceedings.
- [17] M. Beneke *et al.*, “Next-to-Leading Order QCD Corrections to the Lifetime Difference of B_s Mesons”, Phys. Lett. B **459**:631 (1999), [hep-ph/9808385].
- [18] S. Eidelman *et al.* (Particle Data Group), “Review of particle physics”, Phys. Lett. B **592**, 1 (2004); 2005 web-update at <http://pdg.lbl.gov/>.
- [19] Heavy Flavor Averaging Group, <http://www.slac.stanford.edu/xorg/hfag/>.
- [20] G. Buchalla and A. J. Buras, “QCD corrections to rare K and B decays for arbitrary top quark mass”, Nucl. Phys. B **400**:225 (1993).
- [21] A. J. Buras, “Relations between $\Delta M_{s,d}$ and $B_{s,d} \rightarrow \mu\bar{\mu}$ in models with minimal flavour violation”, Phys. Lett. B **566**:115 (2003), [hep-ph/0303060].
- [22] R. Dermisek *et al.*, “Dark Matter and $B_s \rightarrow \mu^+\mu^-$ with Minimal SO_{10} Soft SUSY Breaking”, JHEP 0304:037 (2003), [hep-ph/0304101].
- [23] R. Dermisek *et al.*, “Dark Matter and $B_s \rightarrow \mu^+\mu^-$ with Minimal SO_{10} Soft SUSY Breaking II”, JHEP 0509:029 (2005), [hep-ph/0507233].
- [24] D. Auto *et al.*, “Yukawa coupling unification in supersymmetric models”, JHEP 0306:023 (2003), [hep-ph/0302155].
- [25] T. Blazek, S. F. King, and J. K. Parry, “Implications of $B_s \rightarrow \mu^+\mu^-$ in $SO(10)$ -Like Models”, Phys. Lett. B **589**:39 (2004), [hep-ph/0308068].
- [26] S. R. Choudhury and N. Gaur, “Dileptonic decay of B_s meson in SUSY models with large $\tan(\beta)$ ”, Phys. Lett. B **451**:86 (1999), [hep-ph/9810307].
- [27] K. S. Babu and C. F. Kolda, “Higgs-mediated $B^0 \rightarrow \mu^+\mu^-$ in Minimal Supersymmetry”, Phys. Rev. Lett. **84**:228 (2000), [hep-ph/9909476].
- [28] R. Arnowitt *et al.*, “Detection of $B_s \rightarrow \mu^+\mu^-$ at the Tevatron Run II and Constraints on the SUSY Parameter Space”, Phys. Lett. B **538**:121 (2002), [hep-ph/0203069].